

Hyperfine fields for Sn and magnetic moments in Fe/Cr/Sn/Cr multilayers

A. K. Arzhnikov,* L. V. Dobysheva, and D. V. Fedorov

Physical-Technical Institute, Ural Branch of Russian Academy of Sciences, Kirov str. 132, Izhevsk 426001, Russia

V. M. Uzdin

St. Petersburg State University, ICAPE, 14 linia V.O. 29, 199178, St. Petersburg, Russia

(Received 13 March 2003; published 10 July 2003)

The paper is devoted to a theoretical study of the magnetic moments and hyperfine fields in Fe/Cr/Sn/Cr multilayers. The calculations are conducted by the full potential linearized augmented plane wave, atomic sphere approximation screened Korringa-Kohn-Rostoker (SKKR) and full potential SKKR methods. The results obtained are compared with the Mössbauer spectroscopy experiments and the results of other calculations.

DOI: 10.1103/PhysRevB.68.024407

PACS number(s): 75.70.Cn, 71.15.Ap, 73.21.-b

I. INTRODUCTION

Scientific interest in multilayer magnetic systems is determined by both their importance for technical applications and unsolved fundamental problems of the formation of magnetic properties and other physical characteristics in low-dimensional systems. One of the first objects of study was the Fe/Cr multilayer system prepared in the 1980s.¹ Up to now, though, experimental studies have been unable to determine definitely the character of the magnetic order in Cr multilayers. Recently the authors of Ref. 2 succeeded in obtaining Fe/Cr and Cr multilayer systems with a Sn monolayer inserted. The systems Cr/Sn and Fe/Cr/Sn/Cr were investigated with different physical techniques including the Mössbauer spectroscopy. The main results were the detection of a hyperfine field (HFF) at Sn nuclei and the dependence of its magnitude on the Cr layer thickness. The HFF changes from 2 to 10 T with the Cr thickness changing from 1 to 8 nm. The authors attributed these variations to the magnitude of the magnetic moment at the Cr atom closest to the Sn atom; that is, they supposed that the magnetic moment sharply decreased with the decrease of thickness. The Mössbauer experiments cannot directly answer the question about the character of the magnetic structure and the magnitude of the Cr magnetic moments. That is why the first-principles calculations of the electron structure are a good addition to experiment.

As soon as the experimental data had been available, theoretical first-principles calculations of the electron structure and magnetic characteristics of Fe/Cr/Sn/Cr and Cr/Sn multilayers were conducted.³⁻⁵ The authors asserted that their results agreed, to a certain extent, with experiment, and allowed that the magnetic moment of the Cr atoms are proportional to the HFF at Sn atoms when interpreting experimental results. After a comparison of all the results of Refs. 3 and 4, however, some questions appeared.

(a) The magnitude of Cr magnetic moments in Fe₃/Cr₃/Sn/Cr₃ in Ref. 3 ($-0.19\mu_B$, $0.01\mu_B$ and $-0.11\mu_B$) is much smaller than that in Fe₉/Cr₃/Sn/Cr₃ in Ref. 4 ($-0.70\mu_B$, $0.39\mu_B$, and $-0.61\mu_B$). This looks extremely strange in view of the assertion of Refs. 3 and 4 about a weak effect of the Fe layer thickness on magnetic characteristics.

(b) Relaxation of the magnetic moment magnitude from zero at Sn to high values for bulk Cr is long-distance in Fe₉/Cr₁₄/Sn/Cr₂ (12 layers) and short-distance in Fe₉/Cr₈/Sn/Cr₈ (one layer).⁴

For these reasons we were interested in additional calculations in order to reconcile the results obtained by different methods, to explain the connection between the HFF at Sn nuclei and the magnetic moment magnitude at the nearest Cr atoms and to reveal the characteristic changes of the magnetic moment over the depth of the Cr film in experiment.²

To this aim, we performed calculations of the periodical films Fe/Cr/Sn/Cr and Cr/Sn with different thicknesses of the Fe, Sn, and Cr layers. These first-principles spin-polarized electronic structure calculations are based on spin-density-functional theory in the local-density approximation (LDA). They were conducted by the following methods: full-potential linearized augmented plane wave method (FP LAPW) realized in the program package WIEN2k,⁶ and the screened Korringa-Kohn-Rostoker method developed in Jülich⁷ in the atomic sphere approximation (ASA SKKR) and in the full-potential scheme (FP SKKR). In paper³ the FP LAPW method was used, while in⁴ the tight-binding linear muffin-tin orbital method in the atomic sphere approximation (ASA TB LMTO), that is an approximation of the ASA KKR method. Thus, our calculational methods cover those used in Refs. 3-5, which allows us to compare the results of these papers with ours.

II. MODELS AND CALCULATIONAL METHODS

In our calculations we have used two models. The first was chosen from simple considerations based on the experimental data, that is, the multilayer system was presented as alternating layers in the (001) plane of a bcc lattice. As the lattices of bulk Fe and Cr are close, the Fe-Fe, Fe-Cr, and Cr-Cr interlayer distances are taken equal to 0.144 nm, which corresponds to the half of the lattice parameter of bulk Cr (0.288 nm). The Cr-Sn interlayer distance is chosen in accordance with the experimental data as 0.157 nm.² This model coincide with that of Ref. 4.

Our attempts to obtain the equilibrium position of planes from the calculations of lattice relaxation have given an extremely overestimated value of the Cr-Sn interlayer distance,

TABLE I. The magnetic moments (μ_B) in $\text{Fe}_9/\text{Cr}_3/\text{Sn}/\text{Cr}_3$.

	Fe	Fe	Fe	Fe	Fe	Cr	Cr	Cr	Sn
ASA TB LMTO (Ref. 4)						-0.70	0.39	-0.61	-0.04
ASA SKKR	2.32	2.40	2.38	2.49	1.93	-0.61	0.27	-0.46	-0.02
FP SKKR	2.23	2.30	2.30	2.41	1.91	-0.56	0.28	-0.51	-0.02
FP LAPW	2.26	2.33	2.32	2.43	1.96	-0.55	0.33	-0.55	-0.01

as in Ref. 3, where the Cr-Sn interlayer distance was found to be 0.173 nm. To make a comparison our results with Ref. 3, we have conducted calculations for the second model with the Fe-Fe, Fe-Cr, and Cr-Cr interlayer distances equal to 0.144 nm and the Cr-Sn distance of 0.173 nm.

The distortions of the crystal lattice in the multilayer systems under consideration should be studied carefully, as done in Ref. 5. The lattice relaxation is rather sensitive to the choice of approximation and calculation method; however, we found that the distortions do not essentially affect the character of the Cr magnetic moment variations over the film depth and its dependence on the Cr thickness.

The $\text{Fe}_9/\text{Cr}_3/\text{Sn}/\text{Cr}_3$, $\text{Fe}_9/\text{Cr}_8/\text{Sn}/\text{Cr}_8$, $\text{Fe}_9/\text{Cr}_{14}/\text{Sn}/\text{Cr}_2$, $\text{Fe}_4/\text{Cr}_2/\text{Sn}/\text{Cr}$, $\text{Fe}_8/\text{Cr}_3/\text{Sn}_2/\text{Cr}_3$, $\text{Fe}_3/\text{Cr}_3/\text{Sn}/\text{Cr}_3$, and Cr_3/Sn systems were calculated in the first model, and $\text{Fe}_3/\text{Cr}_3/\text{Sn}/\text{Cr}_3$ and Cr_3/Sn were calculated also in the second model.

The FP LAPW calculation is conducted in a scalar-relativistic approximation for the valence electrons and fully relativistic approximation for the core electrons which are separated by an energy of 7 Ry. The basis of wave functions is restricted by the parameter $R_{MT}^*K_{max}=7$ and the expansion of wave functions over spherical harmonics is limited by a maximum angular momentum equal to 10. The calculations are conducted within the LDA of Perdew and Wang,⁸ as the usually more correct generalized gradient approximation⁹ is known to overestimate the magnetic moments for Cr atoms. The value of the largest vector equal to $G_{max}=20$ is used in the Fourier expansion of the charge density.

For the SKKR calculation a screening potential with a barrier height of 4 Ry is used, and the structure constants include coupling to the next six nearest neighbors. The calculations employ the exchange-correlation potential in the LDA of Vosko, Wilk, and Nusair.¹⁰ An angular momentum cutoff of $l_{max}=3$ is used for the Green function, thus implying a cutoff for the charge density (in the case of the ASA and FP calculations) and potential (in the case of the FP calculations) components at $2l_{max}=6$. The shape of the Voronoi cells for the FP calculations is described by the

proper shape functions expanded up to $4l_{max}=12$. The energy integration is performed by means of a Gaussian quadrature, with 33 points on a semicircle.

We should mention that the meaning of the term ‘‘magnetic moment of atom’’ is slightly different in these methods. In the FP LAPW method the magnetic moment is a result of the integration of the spin density over a nonoverlapping muffin-tin sphere of a certain radius; in the ASA SKKR method the volume of integration sphere is equal to the Voronoi polyhedron for each atom; and in the FP SKKR method the integration is performed over Voronoi polyhedrons.

III. A COMPARISON OF RESULTS OBTAINED BY DIFFERENT CALCULATIONAL METHODS

Tables I, II, III, IV, and V give comparative results for the systems $\text{Fe}_9/\text{Cr}_3/\text{Sn}/\text{Cr}_3$, $\text{Fe}_9/\text{Cr}_8/\text{Sn}/\text{Cr}_8$, $\text{Fe}_9/\text{Cr}_{14}/\text{Sn}/\text{Cr}_2$, $\text{Fe}_3/\text{Cr}_3/\text{Sn}/\text{Cr}_3$, and Cr_3/Sn . First of all, we should note a feature which essentially distinguishes our results from the previous ones in Refs. 3 and 4. Using the SKKR method we have found two solutions in the $\text{Fe}_9/\text{Cr}_{14}/\text{Sn}/\text{Cr}_2$ system which we call ‘‘low spin’’ and ‘‘high spin.’’ The difference in Cr magnetic moment between the two solutions is shown in Fig. 1.

The difference in total energy between the solutions does not exceed 1 mRy in both ASA SKKR and FP SKKR methods, and is smaller than the accuracy of the approximations made in the calculational scheme and in the model. So, for example, the spin-orbit interaction whose magnitude is higher than the difference obtained, lowers the energy of the high-spin state (we have calculated the energy of spin-orbit interaction by the FP LAPW method in $\text{Fe}_3/\text{Cr}_3/\text{Sn}/\text{Cr}_3$, it amounts 1 mRy per atom). Allowance for this interaction within the framework of the SKKR method cannot, however, be made at present.

We did not succeed in finding the second low-spin state in $\text{Fe}_9/\text{Cr}_{14}/\text{Sn}/\text{Cr}_2$ by the FP LAPW method. We could not also find an additional solution in other systems by FP

TABLE II. The magnetic moments (μ_B) at Cr atoms in $\text{Fe}_9/\text{Cr}_8/\text{Sn}/\text{Cr}_8$.

	Cr next to Fe	Cr	Cr	Cr	Cr	Cr	Cr	Cr next to Sn
ASA TB LMTO (Ref. 4)	-0.70	0.59	-0.56	0.59	-0.52	0.51	-0.36	0.56
FP LAPW	-0.57	0.50	-0.52	0.58	-0.55	0.59	-0.49	0.69

TABLE III. The magnetic moments (μ_B) in $\text{Fe}_9/\text{Cr}_{14}/\text{Sn}/\text{Cr}_2$.

	ASA TB LMTO ⁴	ASA SKKR	ASA SKKR	FP SKKR	FP SKKR	FP LAPW
		low-spin	high-spin	low-spin	high-spin	high-spin
Fe		2.33	2.33	2.23	2.23	2.29
Fe		2.40	2.40	2.31	2.31	2.37
Fe		2.38	2.38	2.30	2.30	2.37
Fe		2.47	2.47	2.40	2.41	2.43
Fe		1.99	2.02	1.97	2.00	2.06
Cr	-0.62	-0.53	-0.62	-0.52	-0.64	-0.64
Cr	0.54	0.39	0.51	0.41	0.55	0.58
Cr	-0.52	-0.38	-0.51	-0.41	-0.56	-0.61
Cr	0.55	0.38	0.53	0.43	0.61	0.65
Cr	-0.48	-0.35	-0.52	-0.40	-0.60	-0.64
Cr	0.44	0.31	0.51	0.37	0.60	0.65
Cr	-0.39	-0.30	-0.49	-0.35	-0.59	-0.64
Cr	0.34	0.26	0.48	0.31	0.59	0.66
Cr	-0.28	-0.24	-0.46	-0.28	-0.57	-0.63
Cr	0.21	0.19	0.44	0.24	0.58	0.67
Cr	-0.17	-0.18	-0.43	-0.22	-0.55	-0.63
Cr	0.11	0.14	0.43	0.19	0.58	0.68
Cr	-0.08	-0.09	-0.34	-0.14	-0.48	-0.56
Cr	0.17	0.11	0.45	0.20	0.69	0.80
Sn	0.03	0.01	0.02	0.01	0.02	0.00
Cr	0.60	0.45	0.60	0.49	0.67	0.68
Cr	-0.57	-0.67	-0.76	-0.66	-0.76	-0.73
Fe		2.11	2.13	2.09	2.11	2.12
Fe		2.40	2.41	2.33	2.34	2.40
Fe		2.38	2.38	2.30	2.31	2.38
Fe		2.39	2.39	2.29	2.30	2.35

LAPW or SKKR methods, though we repeatedly attempted to do this by changing the starting density (LAPW) and potential (SKKR) and mixing schemes in the self-consistent procedure. The solutions obtained for $\text{Fe}_9/\text{Cr}_3/\text{Sn}/\text{Cr}_3$ (Table I), $\text{Fe}_3/\text{Cr}_3/\text{Sn}/\text{Cr}_3$ (Table IV), and Cr_3/Sn (Table V) by the FP LAPW and FP SKKR methods agree with each other very well. A good agreement between the high-spin

solution in FP SKKR and in FP LAPW method is also achieved for the $\text{Fe}_9/\text{Cr}_{14}/\text{Sn}/\text{Cr}_2$ system (Table III). The solution found for this system in paper⁴ undoubtedly corresponds to the low-spin one (Fig. 1). We would like to note that the overestimated value of the Cr magnetic moment near Fe is characteristic of ASA TB LMTO calculations (Tables I and II). That is why we classify this solution as a low-spin

TABLE IV. The magnetic moments (μ_B) in $\text{Fe}_3/\text{Cr}_3/\text{Sn}/\text{Cr}_3$, the values in brackets give the Cr-Sn interlayer distance (nm).

	Fe	Fe	Cr	Cr	Cr	Sn
FP LAPW (Ref. 3)(0.173)	2.56	1.70	-0.19	0.01	-0.11	0.00
FP LAPW(0.173)	2.52	1.88	-0.50	0.34	-0.56	-0.002
FP SKKR(0.173)	2.50	1.82	-0.52	0.29	-0.52	-0.017
ASA SKKR(0.173)	2.59	1.84	-0.54	0.29	-0.46	-0.014
FP LAPW(0.157)	2.50	1.88	-0.62	0.37	-0.56	-0.009

TABLE V. The magnetic moments (μ_B) at the Cr atoms and the hyperfine field (T) at the Sn nuclei in Cr_3/Sn , the values in brackets give the Cr-Sn interlayer distance (nm).

	Cr center	Cr next to Sn	HFF_{Sn}
FP LAPW (Ref. 3)(0.173)	0.86	-1.20	28.7
FP LAPW (0.173)	0.72	-1.07	24.9
FP LAPW (0.157)	0.56	-0.91	20.5

one, in spite of its partial coincidence with the high-spin one near Fe atoms. We do not know whether it is possible to obtain the high-spin state in the ASA TB LMTO method, most probably so.

Table IV gives the results of calculation for the $\text{Fe}_3/\text{Cr}_3/\text{Sn}/\text{Cr}_3$ system. One can see a large difference between the results obtained in Ref. 3 and ours. It is the more so surprising as the results for the Cr_3/Sn system are in reasonable accordance (Table V). One could assume a possibility of existence of a second low-spin solution, as in the $\text{Fe}_9/\text{Cr}_{14}/\text{Sn}/\text{Cr}_2$ system, but we could not find it. So, we should conclude that the result obtained in³ for the $\text{Fe}_3/\text{Cr}_3/\text{Sn}/\text{Cr}_3$ system with small magnetic moments at the Cr atoms is not confirmed by either our calculations or those of other authors.⁴

IV. Cr MAGNETIC MOMENT AND ITS RELATION TO THE HFF AT Sn

When discussing the magnetic characteristics of the multilayers under study, we will base ourselves on the FP LAPW calculations. This is due to the fact that the WIEN2K package makes it possible to obtain the hyperfine magnetic field (HFF). Moreover, we have shown that all the FP LAPW results are in a good accordance with the FP SKKR ones. An exception is the low-spin solution in the $\text{Fe}_9/\text{Cr}_{14}/\text{Sn}/\text{Cr}_2$ system that we found by SKKR and did not find by the FP LAPW method. We do not consider it at present believing

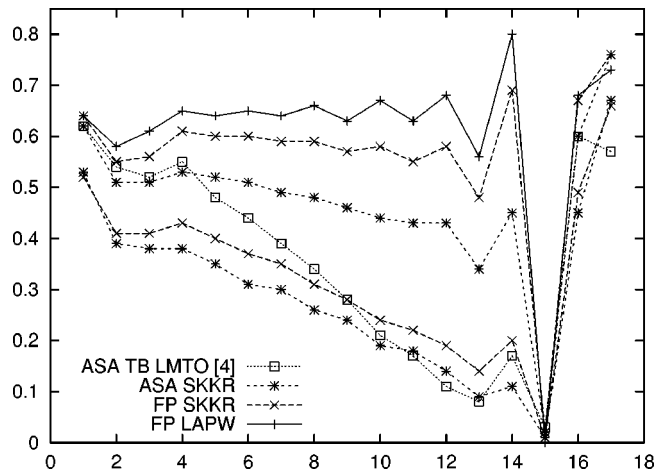


FIG. 1. The magnetic moment magnitude at Cr atoms in the $\text{Fe}_9/\text{Cr}_{14}/\text{Sn}/\text{Cr}_2$ system as a function of the layer number (counted from the Fe layers, the 15th layer being Sn).

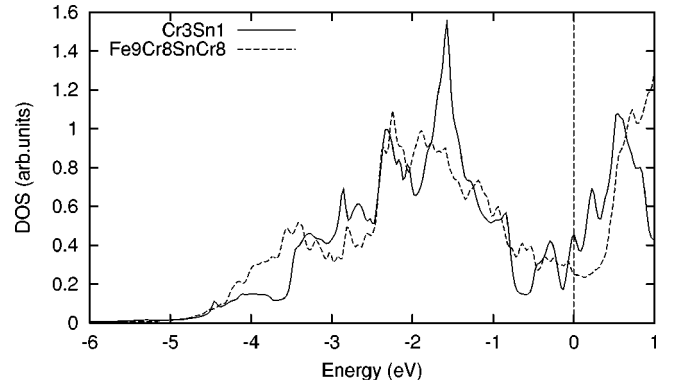


FIG. 2. The density of states of d-electrons with spin up at the Cr atoms in the center of Cr_3/Sn and at the second from the Fe layers Cr in $\text{Fe}_9/\text{Cr}_8/\text{Sn}/\text{Cr}_8$.

it to be more unfavorable in energy due to the spin-orbit interaction.

With the distance to the Cr film, the Fe magnetic moment changes typically for all systems with relatively small variations of its magnitude, see, for example, Tables I, II, III, and IV. The behavior of the magnetic moment at Cr seems to be more complicated than at Fe atoms. However, the situation becomes clear if the effect of Fe and Sn on Cr is considered separately. In the first case, the tails of Fe d-electron states are hybridized with the Cr d electrons of the corresponding spin direction. As the states under the Fermi level at Fe atoms have a preferred spin direction, the effect of hybridization on the electron states of Cr atoms with this spin direction will be greater than on the states with the opposite spin direction. The hybridisation makes bands wider and flatter (Fig. 2), and dependence of this effect on the spin direction results in a decrease of the magnetic moments of Cr atoms with the moment parallel to Fe. This decrease may be observed for all the second Cr atoms if counting from Fe (Tables I, II, III, IV, V, VII, and VIII). This influence spreads out to more distant Cr atoms, but fades rather quickly. Evidently, the influence of the Fe d electron tails is limited to 2–3 atomic layers Fe nearest to Cr, which manifests itself in a weak dependence of the Cr magnetic moments on the Fe film thickness (Fig. 3).

The Sn atoms affect the magnetic moment formation in a different way. The break of the d electrons links at Sn results in a growth of the magnetic moments; the change of the potential near the magnetic atom leads to additional *sp-d* hybridization and a decrease in magnetic moment.¹¹ This

TABLE VI. The magnitude of hyperfine field (T) at Sn nuclei in dependence of the magnitude of magnetic moments (μ_B) at neighboring Cr and at Sn atoms (FP LAPW).

	M_{Cr}	M_{Sn}	HFF_{Sn}	M_{Cr}
$\text{Fe}_3/\text{Cr}_3/\text{Sn}/\text{Cr}_3$	0.56	0.009	11.3	0.56
$\text{Fe}_9/\text{Cr}_3/\text{Sn}/\text{Cr}_3$	0.55	0.007	11.8	0.55
$\text{Fe}_9/\text{Cr}_8/\text{Sn}/\text{Cr}_8$	0.69	0.006	15.4	0.69
$\text{Fe}_9/\text{Cr}_{14}/\text{Sn}/\text{Cr}_2$	0.80	0.004	18.5	0.68
Cr_3/Sn	0.91	0.007	20.5	0.91

TABLE VII. The magnetic moments (μ_B) at magnetic atoms and the hyperfine field (T) at the Sn nuclei in $\text{Fe}_8/\text{Cr}_3/\text{Sn}_2/\text{Cr}_3$.

	Fe	Fe	Fe	Fe	Cr	Cr	Cr	HFF _{Sn}
FP LAPW	2.32	2.35	2.44	1.96	-0.43	0.25	-0.24	8.3

competition defines the final value of the magnetic moment at Cr near the Sn layer. If there is only one Sn layer, the magnetic moment of the closest Cr is greater. In the case of two Sn layers, the hybridization prevails and the magnetic moment decreases (Table VII). We should note that this effect does not depend on the magnetic moment direction.

The interference of the two edge effects from both the Fe and Sn layers results sometimes in a complicated but generally understandable picture of the formation of the magnetic moment at Cr atoms.

Due to the Fe influence, we have reasons to expect a decrease of the magnetic moment with the decrease of the Cr film thickness. This may be clearly seen in the FP LAPW calculations of $\text{Fe}_9/\text{Cr}_3/\text{Sn}/\text{Cr}_3$ (the magnetic moment of the Cr next to Sn is $0.55\mu_B$, Table I) and $\text{Fe}_9/\text{Cr}_8/\text{Sn}/\text{Cr}_8$ (the magnetic moment is $0.69\mu_B$, Table II).

The Mössbauer experiments give the magnitude of the HFF that depends in a complicated way on the space distribution of the magnetic moment. So, it is important to know to what extent we can base ourselves on the experimental data for interpretation of the magnetic moment behavior. As mentioned, the WIEN2K program package allows us to calculate the HFF. The calculated values of the HFF at Sn nuclei are much higher than the experimental ones. This is characteristic of all the existing calculational schemes.^{12,13} The causes of this discrepancy are not clear as yet; however, the obtained dependences of the HFF changes with chemical composition, crystal lattice and so forth, are in a rather good agreement with experimental data, see, for example, Refs. 13 and 14.

First of all, let us discuss the proportionality between the total spin polarization at Sn atom and the HFF at Sn nuclei. Table VI gives the data of calculations of different systems. One can see that no correlation exists between the magnetic moment and the HFF at Sn. At the same time we must conclude that there is a correlation between the HFF at Sn nuclei and the magnetic moment at the closest Cr that allows us to draw qualitative conclusions on the local magnetic moment variations from the HFF at Sn. This, however, should be done with care, because under certain circumstances the spin density oscillations from the second and third neighbors of the Sn atoms may prevail. Table VIII gives the results for the $\text{Fe}_4/\text{Cr}_2/\text{Sn}/\text{Cr}$ system where the magnetic moments of the atoms closest to Sn are oppositely directed. The large value

TABLE VIII. The magnetic moments (μ_B) at magnetic atoms and the hyperfine field (T) at the Sn nuclei in $\text{Fe}_4/\text{Cr}_2/\text{Sn}/\text{Cr}$.

	Fe	Fe	Cr	Cr	HFF _{Sn}	Cr	Fe	Fe
FP LAPW	2.38	2.14	-0.63	0.44	12.4	-0.72	2.09	2.49

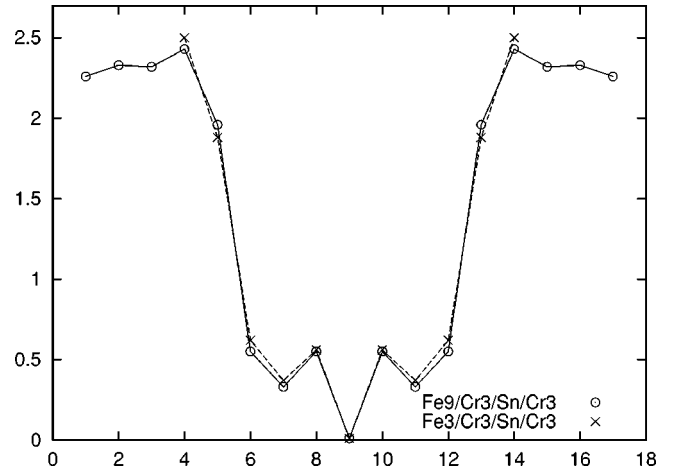


FIG. 3. The magnetic moment magnitude (μ_B) at atoms in $\text{Fe}_9/\text{Cr}_3/\text{Sn}/\text{Cr}_3$ and $\text{Fe}_3/\text{Cr}_3/\text{Sn}/\text{Cr}_3$ (the ninth layer is Sn).

of the HFF at Sn is due to the Fe atoms that are in the second coordination sphere.

Although the allowance for relaxation of the lattice parameter that was mentioned in Sec. II changes the magnitude of Fe and Cr magnetic moment and HFF at Sn (15–20%), it does not change the tendency of their behavior. We can see this from Tables IV and V, where data for two different Cr-Sn interlayer distances (0.157 and 0.173 nm) are given.

V. CONCLUSION

The first-principles calculations of Fe/Cr/Sn/Cr systems by the FP LAPW and (FP, ASA) SKKR methods allow us to make the following conclusions. The calculations by FP SKKR and FP LAPW methods agree well for all the systems investigated with the exception of a low-spin solution in $\text{Fe}_9/\text{Cr}_{14}/\text{Sn}/\text{Cr}_2$. Good agreement of the overwhelming majority of solutions ensures the reliability of the results obtained.

In the $\text{Fe}_9/\text{Cr}_{14}/\text{Sn}/\text{Cr}_2$ system, two solutions are found by the SKKR method with a difference in total energy less than 1 mRy. The characteristic difference between these solutions is the high and small values of the Cr magnetic moments. The high-spin solution coincides with that obtained by the FP LAPW method, the low-spin one agrees with that obtained in Ref. 4 by the ASA TB LMTO method. We did not succeed in corroborating the solution obtained in Ref. 3 for $\text{Fe}_3/\text{Cr}_3/\text{Sn}/\text{Cr}_3$ with low Cr magnetic moments and a HFF at Sn by either the FP LAPW or SKKR method.

An analysis of the theoretical data obtained allows us to explain, from the viewpoint of band structure, the decrease of HFF at Sn nuclei and of the magnetic moment of the closest Cr atoms with the Cr film thickness decrease. These variations are determined by the influence of the closest few Fe layers on the Cr magnetic moments. At the same time, the change of HFF by 1.8 times when changing the Cr film thickness from 1.2 nm (eight layers) to 0.43 nm (three layers), found in calculations, does not agree with a sharp drop almost to zero of the HFF at Sn nuclei found experimentally

when changing the Cr thickness from 4 to 0.5 nm.² To explain the experiment, it seems necessary to invoke some additional mechanisms affecting the formation of the Cr magnetic moment and the HFF at Sn nuclei. As pointed out in, Ref. 2, one of the pretenders to this role is the roughness of the Fe-Cr interface. As experiments¹⁵ show, this roughness is rather large. Another attractive idea to be mentioned is the existence of a second, low-spin solution in all the systems under study whose energy reduces with the Cr thickness de-

crease, but we were not able to find a low-spin solution in other systems.¹⁶

ACKNOWLEDGMENTS

One of us (D.V.F.) would like to thank Dr. N. Papanikolaou and Professor I. Mertig for providing a version of the screened KKR code and valuable advice. This work was supported by INTAS, Grant No. 2001-0386, and Russian Fund for Fundamental Researches, Grant No. 03-02-16139.

*Electronic address: arzhnikov@otf.pti.udm.ru

¹P. Grünberg, R. Schreiber, Y. Pang, M.B. Brodsky, and H. Sowers, *Phys. Rev. Lett.* **57**, 2442 (1986).

²K. Mibu, M. Almokhtar, S. Tanaka, A. Nakanishi, T. Kobayashi, and T. Shinjo, *Phys. Rev. Lett.* **84**, 2243 (2000).

³H. Momida and T. Oguchi, *J. Magn. Magn. Mater.* **234**, 126 (2001).

⁴S. Mukhopadhyay and D. Nguyen-Manh, *Phys. Rev. B* **66**, 144408 (2002).

⁵S. Mukhopadhyay, G.P. Das, S.K. Ghosh, A. Paul, and A. Gupta, *J. Magn. Magn. Mater.* **246**, 317 (2002).

⁶P. Blaha, K. Schwarz, G. K. H. Madsen, D. Kvasnicka, and J. Luitz, WIEN2k, An Augmented Plane Wave + Local Orbitals Program for Calculating Crystal Properties (Karlheinz Schwarz, Techn. Universität Wien, Austria, 2001), ISBN 3-9501031-1-2.

⁷N. Papanikolaou, R. Zeller, and P.H. Dederichs, *J. Phys.: Condens. Matter* **14**, 2799 (2002).

⁸J.P. Perdew and Y. Wang, *Phys. Rev. B* **45**, 13 244 (1992).

⁹J.P. Perdew, S. Burke, and M. Ernzerhof, *Phys. Rev. Lett.* **77**, 3865 (1996).

¹⁰S.H. Vosko, L. Wilk, and M. Nusair, *Can. J. Phys.* **58**, 1200 (1980).

¹¹A.K. Arzhnikov and L.V. Dobysheva, *Comput. Mater. Sci.* **24**, 203 (2002).

¹²H. Akai, M. Akai, S. Blugel, B. Drittler, H. Ebert, K. Terakura, R. Zeller, and P.H. Dederichs, *Suppl. Prog. Theor. Phys.* **101**, 11 (1990).

¹³A.K. Arzhnikov and L.V. Dobysheva, *Phys. Rev. B* **62**, 5324 (2000).

¹⁴A.K. Arzhnikov, L.V. Dobysheva, and F. Brouers, *Phys. Solid State* **42**, 89 (2000).

¹⁵K. Ishiji, H. Okuda, H. Hashizume, M. Almokhtar, and N. Hosoi, *Phys. Rev. B* **66**, 014443 (2002).

¹⁶At the time of submitting the paper we had not found a low-spin solution in other systems, but at present we have succeeded in finding such a solution for Fe₉/Cr₈/Sn/Cr₈ with the SKKR.